SIAM J. APPL. MATH.
Vol. 77, No. 1, pp. 26{50

Purely positive dispersion curvature suggests that Kawahara DSWs occurring in (3) with = 1 will be KdV-like and qualitatively similar to those in Figure 1(a), which we indeed nd to be the case (see subsection 4.4). However, when = +1, the curvature of (4)

$$\omega_{kk} = 6k + 20k^3 \tag{5}$$

changes sign at the in ection point $k_i = \sqrt{3/10}$ as depicted in Figure 2(b). Because DSWs are composed of modulated nonlinear waves with a range of wavenumbers from zero at the solitary wave edge to a characteristic, nonzero value at the harmonic edge [14], we expect fundamental di erences in the DSW structure for (3) when = +1. For example, the \classical" KdV DSWs described earlier feature very di erent structure (orientation, polarity) depending on the dispersion curvature. In this work, we aim to resolve the ways in which a single equation exhibiting both signs of dispersion curvature recti es these di erences.

Note that there is another source of nonconvexity in dispersive hydrodynamic systems: a nonconvex, hyperbolic ux. Such a ux is known to give rise to undercompressive shock waves and shock-rarefactions in hyperbolic systems theory and their analogues in dispersive hydrodynamics [13]. In contrast, the problem of nonconvex dispersion has no hyperbolic correlate.

In the remainder of this introductory section, we review some relevant work on DSWs and solitary waves, then provide an overview of this work.

IQalitativelytersiveydrodynamicsersionatsere2nir--(rr)-422(2S)28(har)50(toing)e 20503NLS051 2yper

aorerupersion is in so1(uie-325(iSW)-420(s)-1(oo1(uucture)-325(i)28(hanges))-4217(Empiiscl)-491(ofb
phe

properties of solitary wave solutions of (3), first computed by Kawahara [23]. Distinct structures emerge depending on the choice of the parameter . For = 1, the solitary waves are monotonically decaying from the peak. For = +1, there are nonmonotonically decaying, depression solitary waves for velocities less than $\frac{1}{4}$ that are stable [5]. These oscillatory solitary waves bifurcate from the linear dispersion curve (4) when the phase and group velocities coincide [16]. The equality of phase and group velocities occurs only for nonconvex dispersion *!*. For = +1 and positive velocities, elevation solitary waves exist but are unstable due to a linear resonance [3, 30]. It is the Kawahara equation's nonconvex dispersion that leads to solitary waves embedded in the linear spectrum [31]. As we will demonstrate, nonconvex dispersion yields similarly impactful effects on DSW dynamics.

1.3. Overview of this work. In section 2, we derive the Kawahara equation (3) from a general dispersive Eulerian system via multiple scales perturbation theory as a universal approximate model for weakly nonlinear dispersive waves when the coefficient of third order dispersion is small. The requisite conditions for higher order dispersive effects to be important are identified and the single free parameter in (3) is related to the dispersive parameters of the original Eulerian system. We then consider water waves and nonlinear fiber optics as example dispersive hydrodynamic systems where this multiple scales method can be applied.

Section 3 reviews the numerical and asymptotic computation of Kawahara solitary wave solutions and their corresponding amplitude-speed relations for (3). These solutions are then utilized to help describe the DSWs studied in section 4.

In subsection 4.1, we show that nonconvex dispersion (= +1) and sufficiently large jumps lead to a new coherent structure, a *traveling* DSW (TDSW). The TDSW is characterized by a nonmonotonic, depression solitary wave trailing edge. Rather than complete a full oscillation, the solitary wave is partial and connects to a periodic nonlinear wavetrain. This portion of the TDSW is found to rapidly approach a *genuine traveling wave solution* of the Kawahara equation (3), connecting a constant to a periodic orbit. Approximate and numerical periodic solutions are obtained that yield the TDSW trailing edge speed as a function of jump height. The speed is found to be a generalization of the Rankine{Hugoniot jump condition of classical shock theory. The TDSW leading edge is found to move with the linear group velocity.

Small jumps for nonconvex dispersion, examined in subsection 4.2, involve long waves and weak fifth order dispersive effects. The resulting DSWs are perturbations of KdV-like DSWs with a leading edge elevation solitary wave that is in resonance with short, forward-propagating linear waves. These are referred to as *radiating* dispersive shock waves (RDSWs). RDSW properties are determined by DSW fitting theory.

Moderate jumps for nonconvex dispersion are examined in subsection 4.3, where more complex dynamics are observed. This is the regime that straddles the linear dispersion inflection point k_{i}, corresponding to unsteady, crossover behavior where we observe strong forward and backward propagation of waves. We equate this regime with wave speeds in the solitary wave \band gap" where Kawahara solitary waves do not exist but nonlinear periodic traveling waves do.

Convex dispersion (= 1) is considered in subsection 4.4, where we observe a classical KdV-like DSW. We apply DSW fitting theory in order to determine the amplitude and speed of the trailing solitary wave and the wavenumber at the leading edge as a function of the initial jump height.

Finally, we conclude the manuscript in section 5 with some discussion and broader perspectives on our findings.

2. Universality of the Kawahara equation. We consider a general dispersive Eulerian system of equations given in nondimensional form by

$$\rho_t + (\rho u)_x = D_1[\rho, u]_x, \tag{6}$$

$$(\rho u)_t + \left(u^2 + P(\rho)\right)_x = D_2[\rho, u]_x, \tag{7}$$

where $\rho = \rho(x,t)$ corresponds to the fluid density and $u = u(x,t)$ the fluid velocity, and the pressure law is given by $P(\rho)$. We assume strict hyperbolicity $P'(\rho) > 0$ and genuine nonlinearity $[\rho^2 P'(\rho)]' > 0$ of the dispersionless system ((6), (7) with $D_{1,2} = 0$) so that weakly nonlinear dynamics exhibit quadratic, convex flux [13]. The differential operators D_1, D_2 acting on ρ, u in (6) and (7) are assumed to be of the second order or higher, yielding a real valued dispersion relation. The dispersion is calculated by assuming a small amplitude linear wave oscillating about the background state (ρ_0, u_0): $\rho = \rho_0 + Ae^{i\theta}$, $u = u_0 + Be^{i\theta}$, where $\theta = kx - \omega t$ and $|A|, |B| \ll 1$ are of the same order. Substitution of this ansatz into (6) and (7) yields a homogeneous system of linear equations for A and B that are only solvable for two distinct frequency branches $\omega = \omega(k)$, the dispersion relation. The dispersion relation is assumed to exhibit the long wave ($0 < k \ll 1$) behavior

$$\omega(k) = u_0 k - c_0 k + \alpha k^3 + \beta k^5 + o(k^5), \tag{8}$$

where $c_0 = \sqrt{P'(\rho_0)}$ is the long wave speed of sound and α, β are the third and fifth order dispersion coefficients, respectively. In general, these coefficients will depend on ρ_0, u_0

Equation (11) can be put in the normalized form (3) by use of the scaled variables

(12) $$x' = \frac{x}{\tilde{\ell}^{1/2}} \quad ; \quad t' = \frac{t}{\tilde{\ell}^{5/2}} \quad ; \quad u' = \frac{u}{\tilde{\ell}^{2}};$$

When $B < 1/3$, gravity effects dominate surface tension effects and we have $\alpha = +1$. Neglecting the fifth order term, the KdV equation (1) therefore exhibits negative dispersion with positive polarity and orientation DSWs as in Figure 1(b).

If we had neglected the higher order terms from the egSerre equations and just used the gSerre equations, the dispersion would not agree with the long wave expansion for the full water waves dispersion relation (16) to fifth order. As such, it is necessary for one to include *both* the effects that result in small third order dispersion as well as higher order terms to maintain the required asymptotic balance. This suggests that one should consider with some caution the applicability of the gSerre model to physical water wave problems when B is near $\frac{1}{3}$.

In [20], the authors derived the Kawahara equation directly from the Euler equations as a5 Td [391(svion)-4(svshn)-oe sv1(l)-441(w)28(ater)-334(w)28(a)27(v(svion)-4(svBons)-4(sv-333(um333(b-440(di)-4
1

Interestingly, a nonzero background velocity u_0 is required in order to achieve a balance between third and fth order dispersion. We note that the numerical simulations in [6] consider the cases $_0 = 0{:}5$, u_0 2 (0:586; 0:543), and $_3$ 2 (1; 0:35), corresponding to = sgn = +1, the nonconvex dispersion case.

2.3. Other systems. The Kawahara equation (3) was derived in the case of intense light propagation through nematic liquid crystals [15]. The governing equation is a nonlocal NLS-type equation. The authors numerically observed the generation of the crossover regime (see subsection 4.3) and related its qualitative features to those of the full model equations, where a more detailed numerical and asymptotic analysis were carried out.

We also note that, with the development of spin-orbit coupled Bose{Einstein condensates (BECs) [24, 25], it is possible to \engineer" the dispersion experienced by the wave functions of two nonlinearly coupled spin states. In a cigar-shaped trap where the BEC is approximately one-dimensional, the mean- eld dynamics may be modeled by two coupled NLS equations (see, e.g., [1] and references therein), which exhibit nonconvex dispersion.

Another novel application of the Kawahara equation is in the description of shallow water waves under ice cover when the Young modulus of ice is su ciently large [21, 28].

3. Solitary wave solutions. The structure of solitary wave solutions to the Kawahara equation (3) is well known [3, 16, 23]. In what follows, we outline relevant properties of these solutions. When = +1, solitary waves are unstable when embedded in the continuous spectrum, i.e., when they exhibit a linear resonance for velocities $c > 0$ [31]. However, there are stable, nonmonotonic solitary waves outside the continuous spectrum when $c < \frac{1}{4}$ [5]. Our investigation of solitary wave solutions focuses upon their numerical and asymptotic calculation. A key quantity of interest is the amplitude-speed relation for these solitary waves, which will prove useful in the study of DSWs.

We seek solutions of (3) in the form $u(x;t) = f(;c)$, $= x \quad ct$. Upon integrating once, we obtain

$$cf + \frac{1}{2}f^2 + \quad f'' + f^{(4)} = 0; \tag{19}$$

where decay of $f(;c)$ and its rst four derivatives eliminates the integration constant. The nonlinear equation (19) is solved via the Newton conjugate gradient method [33] or with the MATLAB boundary value solver bvp5c for the solitary wave pro le f corresponding to the speed c. For comparative purposes, we recall the well-known soliton solution of the KdV equation (1)

$$f(;c) = a \ \operatorname{sech}^2\left(\sqrt{\frac{jaj}{12}} \ ; \quad c(a) = \frac{a}{3}: \right) \tag{20}$$

The monotonic Kawahara solitary waves are well-approximated by the KdV solution (20) in the small amplitude regime [3]. Here, monotonic refers to the decay pro le on either side of the solitary wave peak (a convention presented in [23]. Higher order dispersion acts as a small perturbation to the KdV solitary wave. This a5 2

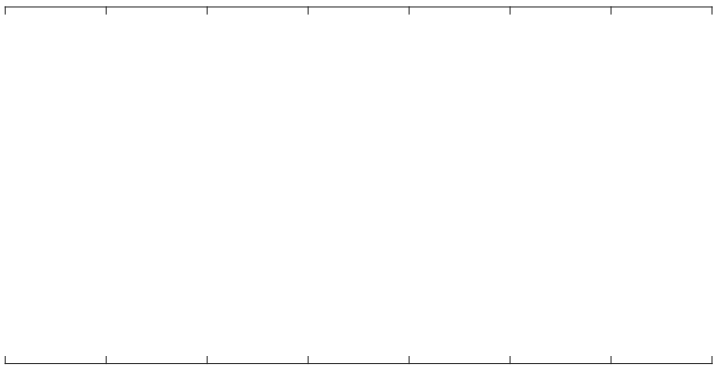

Fig. 3. *Solitary wave pro les and speed-amplitude relation for the Kawahara equation with* = 1 *(solid) and KdV equation (dashed).*

Evaluating at the solitary wave extremum = 0 yields the correction to the KdV speed-amplitude relation (20)

$$c(a) = \frac{a}{3} \quad \frac{f''(0;c)}{a}^{2} = \frac{a}{3} \quad \frac{a^2}{36} + O(a^3): \tag{22}$$

The approximate expression is obtained by inserting the KdV soliton solution (20). The speed correction in (22) is strictly negative, independent of .

The Kawahara solitary wave amplitude-speed relation and sample solitary waves for the case of convex dispersion = 1 are shown in Figure 3.

In the regime of nonconvex dispersion, = +1, there are two distinct branches of solitary wave solutions depicted in Figure 4. The case $c > 0$ corresponds to KdV-like elevation waves. We note that the Kawahara speed-amplitude relation for = +1 more rapidly departs from the KdV relation in Figure 4 than in Figure 3 for = 1. These solutions are embedded in the continuous wave spectrum, consisting of all possible linear phase velocities $!=k = k^2 + k^4 > \frac{1}{4}$ and depicted on the vertical axis in Figure 4. It was observed in [3] that a resonance between the solitary wave and small amplitude waves with the same phase speed occurs. This radiation decreases the amplitude of the solitary wave core as the solution propagates. This is indicative of a general property of embedded solitary waves [31].

When $c < \frac{1}{4}$, the solitary waves are depression waves with nonmonotonic pro- les. In [5], it was shown that this solution branch is stable. The linearization of the solitary wave equation (19) about zero results in a linear, constant coe cient di erential equation with characteristic roots

$$r^2 = \frac{1 \quad \sqrt{1 + 4c}}{2};$$

that are complex with nonzero real part for $c < \frac{1}{4}$ and purely imaginary for $\frac{1}{4} < c < 0$. Consequently, solitary waves with negative velocity can only exist for $c < \frac{1}{4}$. A more detailed, asymptotic analysis of weakly nonlinear, modulated waves for $0 < \frac{1}{4} \quad c \quad 1$ demonstrates a bifurcation of oscillatory, envelope solitary waves, hence the nonmonotonic pro les in Figure 4 for $c < \frac{1}{4}$ [16, 5]. Our numerical computations

Fig. 4. *Solitary wave pro les and speed-amplitude relation for the Kawahara equation with* = +1 *(solid) and KdV equation (dashed). The linear wave spectrum is denoted on the vertical axis by the thick black curve. The \band gap" where no solitary waves exist is the shaded region.*

yield only nonlinear periodic traveling waves for velocities $\frac{1}{4} < c < 0$ so we call this region the *solitary wave band gap*.

4. Dispersive shock waves. In this section, we study DSWs in the Kawahara equation (3), fundamental coherent structures in dispersive hydrodynamics. Generically, DSWs arise in the long-time evolution of initial data that leads to gradient catastrophe or wavebreaking in the dispersionless limit. The canonical GP problem of dispersive hydrodynamics is to consider the evolution of step initial data

$$u(x;0) = \begin{cases} 0; & x < 0; \\ ; & x \quad 0; \end{cases} \qquad 2 \text{ R}: \tag{23}$$

More general, two-parameter initial conditions can be obtained by utilizing the Galilean invariance of the Kawahara equation. First, we recall the behavior of solutions to the dispersionless Hopf equation (2) with initial data (23). When < 0, a rarefaction weak solution exists and approximates the dispersive hydrodynamics of (3) subject to small dispersive corrections. However, when > 0, the Hopf equation (2) admits a weak discontinuous shock wave solution with shock speed

$$s = \frac{1}{2} \tag{24}$$

deduced from the Rankine{Hugoniot jump conditions. The additional dispersive terms in the Kawahara equation act as a singular perturbation and a di erent approach must be explored.

In what follows, we use careful numerical computations of the GP problem for the Kawahara equation (3) with initial data (23) as one of our analysis tools. Motivated

Fig. 5.

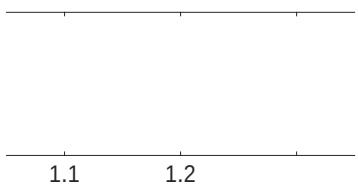

Fig. 8. *Comparison of TDSW harmonic leading edge speed extracted from numerical simula-*

into (19) and carrying out a standard perturbation calculation, we nd

$$F = F_0 + a\cos \quad + a^2 \quad 2c_2 \quad \frac{1}{2F_0} \quad \frac{1}{2 \quad 16k^2 + 64k^4}\cos(2k \ ) \quad + o(a^2); \tag{27}$$

$$c = \frac{F_0}{2} + a^2 c_2 + o(a^2); \tag{28}$$

$$k^2 = \frac{1 + \sqrt{1 \quad 2F_0}}{2}; \tag{29}$$

where

$$c_2 = \frac{3F_0 \quad 16k^2 + 64k^2}{4F_0^2 \quad 64k^2 + 128k^4}; \tag{30}$$

and F_0 is a constant to be determined.

The mean requirement (26) applied to (27) yields

$$F_0 + a^2 \quad 2c_2 \quad \frac{1}{2F_0} \quad = \quad : \tag{31}$$

To account for the $O(a^2)$ terms in the mean, the background F_0 is expanded in the parameter a in the form $F_0 = F_{0;0} + a^2 F_{0;2} + o(a^2)$. Substitution of the asymptotic expansion yields

$$F_0 = \quad \frac{a^2}{2} \quad \frac{29 \quad + 24\sqrt{2 \quad + 1} + 24}{^2 + 16 \quad + 8\sqrt{2 \quad + 1} + 8} + \frac{1}{\quad} \quad ; \tag{32}$$

e ectively canceling the $O(a^2)$ mean terms in (27). The only remaining free parameter is the wave amplitude a, which can be determined by inserting the expansion (27) into the zero energy estimate (21) and evaluating at the wave maximum = 0, which yields

$$a = \sqrt{\frac{}{3 + \frac{9}{2} + 3\sqrt{2 \quad + 1}}}^{3=2}: \tag{33}$$

Combining (32), (30), (29). and (28), we obtain an amplitude correction to the speed of the traveling wave

$$c = \quad \frac{}{2} + \frac{a^2}{4}; \tag{34}$$

and the square wavenumber of the wavetrain at leading order is given by

$$k^2 = \frac{1 + \sqrt{1 + 2 \quad}}{2}: \tag{35}$$

We verify the accuracy of these approximate solutions by directly computing mean , zero energy periodic orbits satisfying (19) and (21) using the MATLAB boundary value solver bvp5c. Figure 9 shows the estimated and computed parameters c, a, and k for mean periodic solutions. Excellent agreement is obtained for all values of for which the traveling wave solutions were calculated.

What we have shown is that if a Kawahara traveling wave satisfying the BCs (25) and (26) exists, its speed c is determined by the BCs and, in particular, the

Fig. 9. *Comparisons of asymptotic predictions of nonlinear wavetrain features:* (a) *the amplitude of the nonlinear wavetrain,* (b) *the square of the wavenumber of the nonlinear wavetrain, and* (c) *the speed of the traveling wave. All gures compare values from computed traveling wave solutions (solid), asymptotic predictions (dashed), and data extracted from numerical simulations of the GP problem (pluses).*

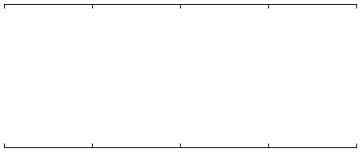

Fig. 10. (a) *Superimposed traveling wave solution to the dynamical system* (19) *with BCs* (36) *(solid) on a TDSW computed from the GP problem with* = 1

We further examine properties of the TDSW by comparing the numerically extracted trailing edge velocity, s , of the TDSW and the speed of the computed traveling wave, c, in Figure 9(a). We also compare the amplitude of the TDSW

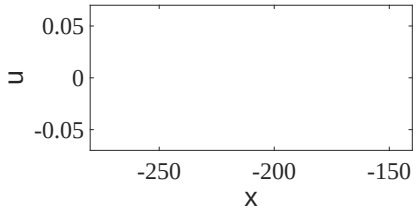

Fig. 11. *Numerically computed Kawahara RDSWs in the small jump regime.* (a) *The solution at t* 8573 *for jump* = 0:06. *The radiation is not visible due to its small amplitude.* (b) *Zoomed-in view of radiation for RDSW in panel* (a). (c) *RDSW leading edge from* (a) *with an overlay of a numerically computed Kawahara solitary wave of the same speed.* (d) *Comparison of the leading edge ampltude* a_+ *versus incorporating predictions from Kawahara DSW tting (solid) and extracted values from numerical simulations (pluses).*

The RDSW trailing edge wavenumber k is characterized by a simple wave so-

Fig. 13. *Crossover Kawahara DSW dynamics for the intermediate jump value* = 0:3 *with* = +1. *Initial data is the dashed curve.*

Figure 11(a). The DSWs for values of in this region are qualitatively characterized by this remnant of a small amplitude RDSW with positive polarity and orientation with superimposed small amplitude waves that suggest incoherence. Such incoherence results in wave mixing that eliminates the rank ordered structure of the RDSWs that occur at smaller jumps. The largest amplitude, elevation wave does not appear to resemble any of the Kawahara solitary waves we have computed in Figure 4 and waves propagate both ahead of and behind the peak. Just as we identify the leading edge of RDSWs resulting from small jumps with elevation solitary waves in Figure 4 ($c > 0$) and the TDSW trailing edge for large jumps with nonmonotonic elevation solitary waves ($c < 1=4$), we interpret the intermediate jump transition region as corresponding to the solitary wave \band gap" for 1=

Fig. 14. *Development of a classical Kawahara DSW with initial jump = 1 and convex dispersion = 1. Approximate initial data is shown in the top gure with the dashed curve.*

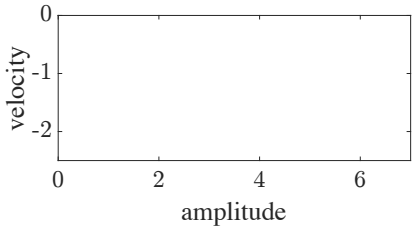

Fig. 15. *Comparison of DSW leading edge properties to Kawahara solitary waves.* (a) *Speed-amplitude relation of Kawahara solitary wave (solid) and DSW trailing edge (pluses) for = +1.* (b) *Overlay of numerically computed solitary wave with coincident velocity with the DSW trailing edge for = 1.*

4.4. Convex dispersion. In the case where the sign of the third order term is negative (= 1), the Kawahara dispersion relation (4) is a purely convex function of k. These are \convex dispersive hydrodynamics" so we expect KdV-like DSWs. For completeness, we brie y analyze this case.

The numerical simulation in Figure 14 depicts the temporal evolution of step initial data (23) for (3). This gure portrays the temporal development of a DSW that is qualitatively similar to the classical KdV DSW. The addition of the fth order term in (3) serves as a perturbation to the KdV equation that, in contrast to the nonconvex case = +1, does not qualitatively change the dynamics. The DSW trailing edge behaves like a solitary wave solution of the Kawahara equation as shown by Figure 15(a), where the DSW trailing edge speed-amplitude relation, extracted from multiple simulations, is compared to the solitary wave amplitude-speed relation from Figure 3. A Kawahara solitary wave of velocity given by the trailing edge is superimposed on the DSW trailing edge in Figure 15(b).

We now implement the DSW tting method [12] (see also [14]). The implementation is essentially the same as that of subsection 4.2 but we now use the dispersion relation (4) and approximate solitary wave amplitude-speed relation (22), both with = 1. We omit the details. The macroscopic DSW harmonic leading edge

Fig. 16. *Kawahara DSW trailing edge wavenumber* (a) *and DSW leading edge speed* (b) *for varying jump height. Comparison between Whitham theory predictions for the Kawahara equation (solid), Whitham theory for the KdV equation (dashed), and numerical simulation (plusses).*

properties are the characteristic wavenumber

$$k_+ = \frac{3 + \sqrt{9 + 20\alpha}}{5}^{1/2} = \frac{2}{3}^{1/2} \frac{5}{9\sqrt{6}}\alpha^{3/2} + O(\alpha^{5/2}) \tag{50}$$

and speed

$$s_+ = \frac{9}{5} + 3\alpha \frac{3}{5}\sqrt{9 + 20\alpha} = \alpha + \frac{10}{9}\alpha^2 + O(\alpha^3); \tag{51}$$

Figure 16(a) shows the DSW harmonic edge wavenumber k_+ versus jump height. DSW fitting theory provides an excellent approximation of the leading edge wavenumber, extracted from our numerical simulations. In particular, DSW fitting correctly captures the reduction of the trailing edge wavenumber relative to the leading order KdV result $k_+ = \sqrt{2\alpha/3}$. We see that higher order dispersion has a significant quantitative effect on the properties of the harmonic wave edge.

The macroscopic properties of the DSW solitary wave trailing edge include the velocity

$$s = \frac{3}{25}\alpha \frac{4}{5} \frac{1}{25}\sqrt{9\alpha^2 - 20\alpha} = \frac{2}{3}\alpha + \frac{2}{27}\alpha^2 + O(\alpha^3) \tag{52}$$

and the amplitude

$$a = 2\alpha^2 \frac{5}{9}\alpha^2 + O(\alpha^3); \tag{53}$$

approximated by using (22) and equating $s = c(a)$. Although the trailing edge velocity is only defined for $0 < \alpha < 9/20$, the small α asymptotics agree with the KdV velocity (and amplitude a_+) to leading order [17]. The next order correction shows that the Kawahara DSW solitary wave edge velocity is above the corresponding KdV DSW velocity, which agrees with the numerical simulations shown in Figure 16(b) for α below the critical value 9/20. The DSW fitting method fails for $\alpha > 9/20$, even though numerical computations show a clear trend.

5. Discussion and conclusion. The Kawahara equation is a universal asymptotic model of weakly nonlinear, dispersive hydrodynamics with higher order dispersion. The classification of the GP initial step problem carried out here reveals classical, KdV-like DSWs when the dispersion is convex and three distinct regimes for nonconvex dispersion. These three regimes represent an intrinsic mechanism for

the transition from convex to nonconvex dispersive hydrodynamics. An example from shallow water waves (recall subsection 2.1) illuminates this transition.

When gravity dominates surface tension e ects, the Bond number B is small so that higher order dispersive e ects continue to yield negative dispersion curvature for all but very short wavelengths (recall (16)). DSWs in this regime are therefore KdV-like, satisfying (1) with $= +1$, with positive orientation and polarity as in Figure 1(b). For B less than but close to 1=3, where surface tension and gravity start to balance, the nonconvexity of the dispersion relation manifests in the Kawahara equation (3) with $= +1$. Small jumps still yield KdV-like DSWs with positive orientation and polarity but now they are accompanied by a resonance and small amplitude forward radiation. These are RDSWs. As the jump height is further increased, the forward radiation gets stronger at the expense of backward wave propagation until a critical jump height is reached. Above this threshold, a TDSW with negative orientation and polarity is generated, exhibiting a steady traveling wave structure at the trailing edge. Thus, the crossover from positive to negative DSW polarity and

The generalized Rankine{Hugoniot condition is a kind of nonlinear resonance condition in the sense that the trailing edge solitary wave velocity coincides with the adjacent periodic traveling wave velocity. Such a condition has been assumed previously [6, 15] but here we show that it is inherent in the generation of a traveling wave structure within the TDSW.

Although a nonconvex dispersion can give rise to TDSWs above threshold, it is not necessary. Another model equation, the conduit equation, also with nonconvex dispersion, does not exhibit such solutions [26]. But that model, a Benjamin{Bona{ Mahony type equation [4] does display nonclassical DSW dynamics at the DSW harmonic wave edge. Likely, the principle reason that TDSWs do not occur is the lack of a linear resonance at the DSW solitary wave edge.

A unique feature of the TDSW is its triple personality. On the one hand, it is similar to a dissipative shock wave in that it satis es a generalized Rankine{Hugoniot condition and exhibits a steady character when viewed near the shock front. On the other hand, the TDSW is similar to a classical DSW, exhibiting two distinct limits: a small amplitude, harmonic edge moving with the group velocity and a large amplitude solitary wave edge moving with the phase velocity. But the TDSW is distinct in that the transition from a periodic wave to a solitary wave occurs almost instantaneously, setting it apart from DSWs in convex dispersive hydrodynamics and shock waves in dissipative hydrodynamics.

Acknowledgment. The authors are grateful to James Meiss for insightful discussions.

REFERENCES

[1] V. Achilleos, D. J. Frantzeskakis, P. G. Kevrekidis, and D. E. Pelinovsky, *Matter-wave bright solitons in spin-orbit coupled Bose-Einstein condensates*, Phys. Rev. Lett., 110 (2013), 264101.

[2] I. Bakholdin, *Non-dissipative Discontinuities in Continuum Mechanics* (in Russian), Fizmalit, Moscow, 2004.

[3] E. Benilov, R. Grimshaw, and E. Kuznetsova, *The generation of radiating waves in a singularly-perturbed Korteweg-de Vries equation*, Phys. D, 69 (1993), pp. 270{278.

[4] T. B. Benjamin, J. L. Bona, and J. J. Mahony, *Model equations for long waves in nonlinear dispersive systems*, Philos. Trans. R. Soc. Lond. Ser. A Math. Phys. Eng. Sci., 272 (1972), pp. 47{78.

[5] D. C. Calvo, T.-S. Yang, and T. Akylas, *On the stability of solitary waves with decaying oscillatory tails*, Proc. R. Soc. Lond. Ser. A Math. (2000), pp. 469{487.

[6] M. Conforti, F. Baronio, and S. Trillo, *Resonant radiation shed by dispersive shock waves*, Phys. Rev. A, 89 (2014), 013807.

[7] M. Conforti and S. Trillo, *Dispersive wave emission from wave breaking*, Opt. Lett., 38 (2013), pp. 3815{3818.

[8] M. Conforti and S. Trillo, *Radiative e ects driven by shock waves in cavity-less four-wave mixing combs*, Opt. Lett., 39 (2014), pp. 5760{5763.

[9] M. Conforti, S. Trillo, A. Mussot, and A. Kudlinski, *Parametric excitation of multiple resonant radiations from localized wavepackets*, Sci. Rep., 5 (2015), pp. 1{5.

[10] F. Dias and P. Milewski, *On the fully-nonlinear shallow-water generalized Serre equations*, Phys. Lett. A, 374 (2010), pp. 1049{1053.

[11] B. Dubrovin, T. Grava, and C. Klein, *Numerical study of breakup in generalized Korteweg-de Vries and Kawahara equations*, SIAM J. Appl. Math, 71 (2011), pp. 983{1008.

[12] G. El, *Resolution of a shock in hyperbolic systems modi ed by weak dispersion*, Chaos, 15 (2005), 37103.

[13] G. A. El, M. A. Hoefer, and M. Shearer, *Dispersive and di usive-dispersive shock waves for nonconvex conservation laws*, SIAM Rev., to appear, arXiv:1501.01681 [nlin.PS].

[14] G. A. El and M. A. Hoefer, *Dispersive shock waves and modulation theory*, Phys. D, 333 (2016), pp. 11{65.

[15] G. A. El and N. F. Smyth, *Radiating dispersive shock waves in non-local optical media*, Proc. R. Soc. Phys. Eng. Sci., 472 (2016).
[16] R. Grimshaw, B. Malomed, and E. Benilov, *Solitary waves with damped oscillatory tails: an analysis of the fth-order Korteweg-de Vries equation*, Phys. D, 77 (1994), pp. 473{485.
[17] A. V. Gurevich and L. P. Pitaevskii, *Nonstationary structure of a collisionless shock wave*, Sov. Phys. JETP, 38 (1974), pp. 291{297.
[18] M. Haragus and G. Iooss, *Local Bifurcations, Center Manifolds, and Normal Forms in In nite-Dimensional Dynamical Systems*, Springer, London, 2011.
[19] M. Hirata, S. Okino, and H. Hanazaki, *Numerical simulation of capillary gravity waves excited by an obstacle in shallow water*, Proc. Est. Acad. Sci., 64 (2015), pp. 278{284.
[20] J. K. Hunter and J. Scheurle, *Existence of perturbed solitary wave solutions to a model equation for water waves*, Phys. D, 32 (1988), pp. 253{268.
[21] A. T. Ilichev and V. Y. Tomashpolskii, *Soliton-like structures on a liquid surface under an ice cover*, Theoret. Math. Phys., 182 (2015), pp. 231{245.
[22] R. S. Johnson, *A Modern Introduction to the Mathematical Theory of Water Waves*, Cambridge University Press, Cambridge, UK, 1997.
[23] T. Kawahara, *Oscillatory Solitary waves in dispersive media*, J. Phys. Soc. Jpn., 33 (1972), pp. 260{264.
[24] Y.-J. Lin, R. L. Compton, K. Jimenez-Garc a, J. V. Porto, and I. B. Spielman, *Synthetic magnetic elds for ultracold neutral atoms*, Nature, 462 (2009), pp. 628{632.
[25] Y.-J. Lin, K. Jimenez-Garc a, and I. B. Spielman, *Spin-orbit-coupled Bose-Einstein condensates*, Nature, 471 (2011), pp. 83{86.
[26] N. K. Lowman and M. A. Hoefer, *Dispersive shock waves in viscously deformable media*, J. Fluid Mech., 718 (2013), pp. 524{557.
[27] S. Malaguti, M. Conforti, and S. Trillo, *Dispersive radiation induced by shock waves in passive resonators*, Opt. Lett., 39 (2014), pp. 5626{5629.
[28] A. Marchenko, *Long waves in shallow liquid under ice cover*, J. Appl. Math, 52 (1988), pp. 180{183.
[29] Y. Matsuno, *Hamiltonian formulation of the extended Green-Naghdi equations*, Phys. D, 301 (2015), pp. 1{7.
[30] Y. Pomeau, A. Ramani, and B. Grammaticos, *Structural stability of the Korteweg-de Vries solitons under a singular perturbation*, Phys. D, 31 (1988), pp. 127{134.
[31] Y. Tan, J. Yang, and D. E. Pelinovsky, *Semi-stability of embedded solitons in the general fth-order KdV equation*, Wave Motion, 36 (2002), pp. 241{255.
[32] G. B. Whitham, *Linear and Nonlinear Waves*, Pure Appl. Math. 42, J Wiley, New York, 2011.
[33] J. Yang, *Newton-conjugate-gradient methods for solitary wave computations*, J. Comput. Phys., 228 (2009), pp. 7007{7024.